

# Attentive Feature Aggregation or: How Policies Learn to Stop Worrying about Robustness and Attend to Task-Relevant Visual Cues<sup>†</sup>

Nikolaos Tsagkas<sup>1,α</sup>, Andreas Sochopoulos<sup>1</sup>, Duolikun Danier<sup>1</sup>,  
Sethu Vijayakumar<sup>1</sup>, Alexandros Kouris<sup>3</sup>, Oisin Mac Aodha<sup>1,ε</sup>, Chris Xiaoxuan Lu<sup>2,ε</sup>  
<sup>1</sup>University of Edinburgh, <sup>2</sup>UCL, <sup>3</sup>Samsung AI Center - Cambridge, UK

**Abstract**— The adoption of pre-trained visual representations (PVRs), leveraging features from large-scale vision models, has become a popular paradigm for training visuomotor policies. However, these powerful representations can encode a broad range of task-irrelevant scene information, making the resulting trained policies vulnerable to out-of-domain visual changes and distractors. In this work we address visuomotor policy feature pooling as a solution to the observed lack of robustness in perturbed scenes. We achieve this via Attentive Feature Aggregation (AFA), a lightweight, trainable pooling mechanism that learns to naturally attend to task-relevant visual cues, ignoring even semantically rich scene distractors. Through extensive experiments in both simulation and the real world, we demonstrate that policies trained with AFA significantly outperform standard pooling approaches in the presence of visual perturbations, without requiring expensive dataset augmentation or fine-tuning of the PVR. Our findings show that ignoring extraneous visual information is a crucial step towards deploying robust and generalisable visuomotor policies.

Project Page: [tsagkas.github.io/afa](https://tsagkas.github.io/afa).

## I. INTRODUCTION

Performing robust and accurate robotic manipulation from visual inputs necessitates informative and stable visual representations. The traditional paradigm for training visuomotor policies has involved learning visual encoders from scratch alongside policy models [27]. Recently, however, the adoption of pre-trained visual representations (PVRs) (*a.k.a.* vision foundation models), *i.e.*, computer vision models trained on large and diverse visual datasets, has emerged as a compelling alternative, moving away from the *tabula-rasa* approach [40], [24], [31], [42], [11], [20]. This shift has been driven mainly by three key factors: the SoTA performance of PVRs in computer vision tasks, their impressive generalisation capabilities derived from training on vast datasets, and the absence of robust robot-specific foundation models [22].

Even though PVRs have played an instrumental role in downstream robotics applications, such as semantic map-

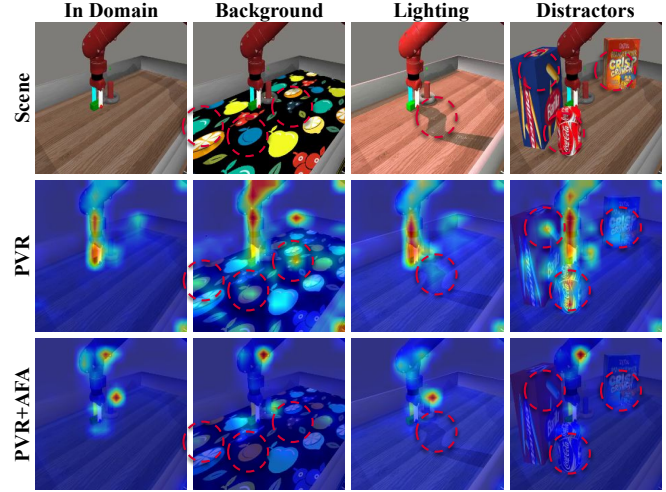


Fig. 1: Comparison of attention heatmaps with and without AFA (PVR: DINO). AFA learns to attend to focused, task-relevant regions, ignoring scene changes (e.g., distractors).

ping [44], [45], language-guided [41], [23] and affordance-guided [25], [28] manipulation, and more, their role in imitation learning can lead to a paradoxical phenomenon. The very PVRs that are selected for their ability to provide descriptive and generalisable features, also encode a broad range of scene information, much of which may be irrelevant to the specific task. As a result, introducing visual changes in the scene, particularly ones with rich semantic meaning—as in Fig. 1—the more likely it is for the policy’s input to be driven out-of-domain (OOD), leading to task failure. This lack of robustness is a well-known problem [48], [16], [4], [19], [29]. Nevertheless, prior works either simply acknowledged and quantified the problem, or proposed solutions that required dataset augmentation [16], [29], a costly approach for real-world robotics applications. In this work, we argue that an effective way of improving the policy’s robustness should leave the PVR out of the fine-tuning loop, which ideally should be kept frozen to avoid diluting the representation. Similarly, the methodology is better to not rely on dataset augmentations, which is difficult and costly to collect in real-world imitation learning. At the same time, dataset enhancements in-simulation require dealing with `sim2real` transfer, a problem that is not trivial to solve. On the contrary,

\*This work was supported by the United Kingdom Research and Innovation (grant EP/S023208/1), EPSRC Centre for Doctoral Training in Robotics and Autonomous Systems (RAS) and ELIAI (Edinburgh Laboratory for Integrated Artificial Intelligence) - EPSRC (EP/W002876/1).

<sup>†</sup>The title is inspired by Stanley Kubrick’s film: “*Dr. Strangelove or: How I Learned to Stop Worrying and Love the Bomb*”.

<sup>ε</sup> Indicates equal senior authorship.

<sup>α</sup> Corresponding author: N. Tsagkas – n.tsagkas@ed.ac.uk

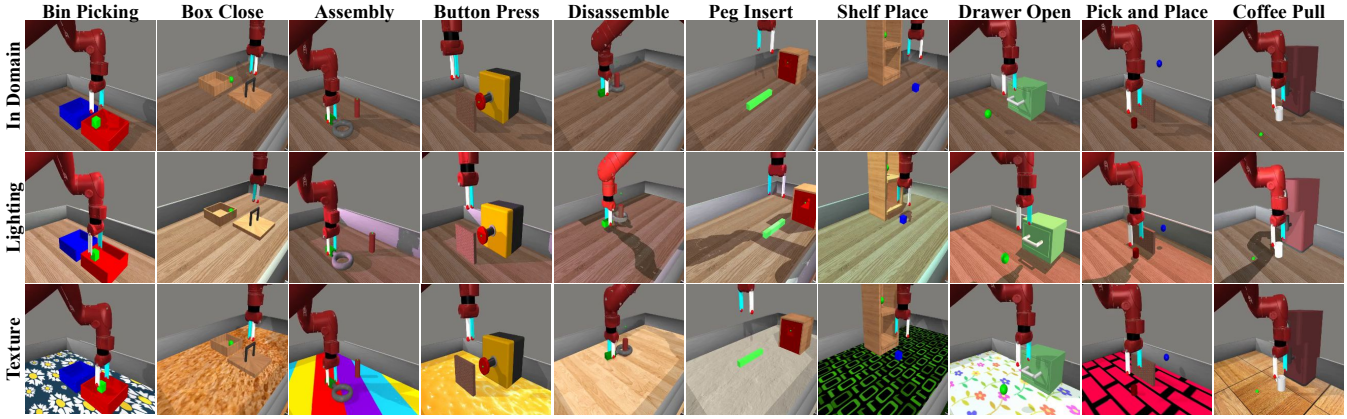


Fig. 2: Visualisation of the tasks used for evaluation. The first row illustrates representative scenes, as seen in the frames from the expert demonstrations (in-domain). The second row shows how the scenes are modified by randomly altering the brightness, orientation and position of the light source. Similarly, the third row presents changes to the tabletop texture.

we propose that the solution should concern the way PVR feature extraction is handled, learning to attend only to task-specific information.

In summary, we make the following contributions:

**1. Re-think visuomotor policy feature pooling.** We propose the use of a trainable module, inspired by recent work in computer vision [7], [10], [1], called *Attentive Feature Aggregation* (AFA), for the purpose of increasing robustness under scene perturbations, by naturally learning to attend to task-relevant visual cues. Our method outperforms greatly standard approaches, while in some cases even triples OOD performance.

**2. Introduce robustness predictors.** We evaluate the use of AFA both in in-domain and OOD scenes, under lighting and background visual perturbations. We validate its superior robustness across 14 popular PVRs and two SoTA pooling approaches, widely adopted in visuomotor policy learning. We further verify AFA’s efficacy in the real-world. From these results, we make an interesting observation, that certain metrics can hint increased OOD performance. More specifically, we find that the amount of attention mass that falls within task-relevant regions and the attention entropy score (*i.e.*, how targeted the attention is) are strongly correlated with the OOD policy performance. AFA improves both metrics, which justifies its increased performance.

## II. RELATED WORK

**Robustness in PVR-based policies:** PVRs are favoured for their generalisation capabilities in vision tasks, but OOD generalisation remains challenging in policy deployment. [48] analysed the impact of various perturbations on PVR-based policy generalisation, while [4] identified correlations between generalisation performance and inherent model traits, such as ViTs’ segmentation ability. Conversely, [16] found that learning from scratch with data augmentation can yield competitive results, while [29] found that adapters [19] can improve policy generalisation when training with diverse object instances. In contrast, we focus on developing

methods that achieve robustness to scene changes without relying on dataset augmentation, which can be prohibitively expensive in real-world robotics applications, or updating the parameters of the PVR, which could harm their generalisation properties.

**Isolating task-relevant features:** Downstream vision tasks often make use of the output features of PVRs (*e.g.*, semantic correspondence [32], depth estimation [50], etc.). However, these features typically encode a broad range of scene information, much of which may be irrelevant to the specific task. To address this challenge, attentive probing [7], [10], [1] has emerged as a popular evaluation technique, leveraging local tokens. This approach employs a cross-attention layer with a trainable query token, treating the local features from PVRs as a sequence of key-value pairs. Unlike traditional evaluation methods such as linear probing (*i.e.*, stacking a linear layer after a pre-trained model to evaluate the capabilities of the output feature on a simple task), attentive probing (*i.e.*, deploying a cross-attention layer with a trainable query token to process the local output features), has shown significantly different vision evaluation outcomes, particularly with PVRs trained using Masked-Image Modelling (MIM) approaches (*e.g.*, MAE [17]), where features, such as the CLS token, often include irrelevant information. Similarly, in robot learning, task-relevant signals like joint angles may correspond to particular image regions, with unrelated cues acting as distractions. In this work, we find that attentive probing is key to robust and generalizable visuomotor policy learning too, where the trainable query token learns to attend to task-relevant visual cues.

**Policy observation pooling:** In robotics applications, the idea of pooling a sequence of observation tokens has been explored, and it is usually deployed for reducing the input stream length. A popular choice remains to this day adding a Spatial Softmax operation between the visual encoder and the policy network [18], [9]. Similarly, RT-1 [3] utilised a TokenLearner [39] for making the policy input more compact, thus speeding up inference time. However, there is no current consensus as to how PVR features can be

effectively used such that the policy model learns to attend only to task-relevant signals, ignoring unrelated cues that act as distractors. By prioritizing task-relevant signals, we show that *Attentive Feature Aggregation (AFA)* enhances task performance in OOD scenarios, outperforming traditional pooling methods. Recently, ICRT [14] also adopted attentive probing in the context of visuomotor policy learning, but for the purpose of learning to project image observations from different views, the robot's proprioception and actions into a joint latent space for conducting sequence modelling. To the best of our knowledge, we are the first to utilise AFA for increasing the policy's robustness.

### III. PRELIMINARIES

#### A. Imitation Learning via Behaviour Cloning

We assume access to an expert policy  $\pi^*$  that prescribes robot actions based on both proprioceptive input  $p \in \mathcal{P}$  and visual input  $o \in \mathcal{O}$ . The output is an action  $a \in \mathcal{A}$ . Executing this controller yields a collection of expert rollouts  $\mathcal{T}^e = \{(p_t^i, o_t^i, a_t^i)_{t=0}^T\}_{i=1}^N$ , where each of the  $N$  trajectories is composed of  $T$  time steps of observations paired with corresponding actions.

The learner's objective is to approximate  $\pi^*$  with a parameterised policy  $\pi_\theta$ . We adopt standard behaviour cloning, in which  $\pi_\theta$  is trained on expert demonstrations by minimizing the squared error between expert actions and the policy's predictions:

$$\mathbb{E}_{(p_t^i, o_t^i, a_t^i) \sim \mathcal{T}^e} \|a_t^i - \pi_\theta(f_{\text{PVR}}(o_t^i), p_t^i)\|_2^2, \quad (1)$$

where the function  $f_{\text{PVR}}$  denotes a fixed PVR that transforms the raw visual stream  $o_t^i$  into global feature vectors (see Fig. 3a).

Following common practice [35], [33], [21], [46], we implement  $\pi_\theta$  as a lightweight multilayer perceptron, with 4 layers, separated by ReLUs, applying a tanh activation at the end to constrain outputs. The policy predicts the mean  $\mu$  of a Gaussian distribution with a fixed variance  $\sigma^2$ , and actions are sampled from a truncated Gaussian  $\mathcal{N}^T(\mu, \sigma^2)$  restricted to the range  $[-1, 1]^k$ , where  $k$  is the dimensionality of the action space.

#### B. Policy Pooling Mechanisms

**Spatial Softmax** has been widely used in visuomotor policy learning [13], [9] for extracting spatially meaningful, compressed features from convolutional feature maps. This pooling method operates by interpreting the activation map as a probability distribution over spatial locations, thereby encouraging the network to focus on the most feature-rich regions in the image. This results in a differentiable way to extract expected spatial coordinates of visual features, which can be directly fed into downstream policy networks.

Given a feature map  $f \in \mathbb{R}^{C \times H \times W}$ , where  $C$  is the number of channels, and  $H, W$  are the height and width respectively, the Spatial Softmax is applied to each channel  $c$  as follows:

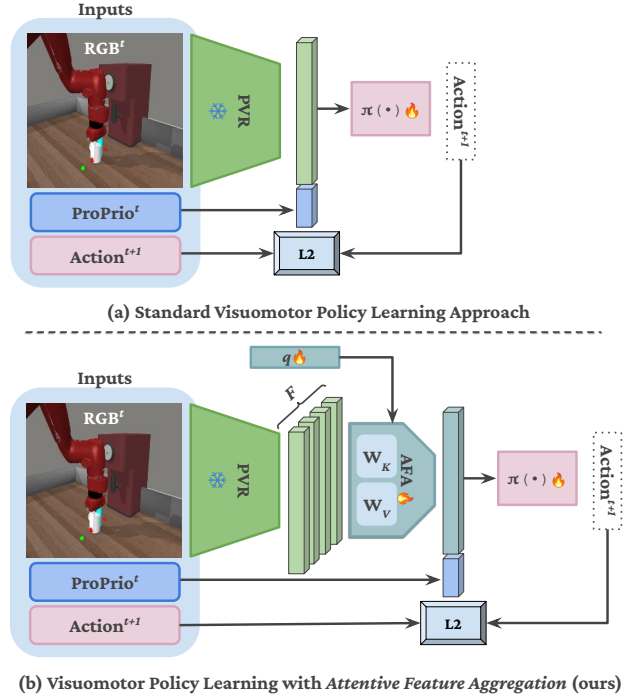


Fig. 3: Visualisation of (a) the standard visuomotor policy learning approach and (b) the proposed approach with AFA.

$$s_{ij}^{(c)} = \frac{\exp(f_{ij}^{(c)})}{\sum_{i'=1}^H \sum_{j'=1}^W \exp(f_{i'j'}^{(c)})} \quad (2)$$

Using the resulting softmax weights  $s_{ij}^{(c)}$ , the expected 2D coordinates  $(\hat{x}^{(c)}, \hat{y}^{(c)})$  for each channel are computed as:

$$\hat{x}^{(c)} = \sum_{i=1}^H \sum_{j=1}^W s_{ij}^{(c)} \cdot x_j, \quad \hat{y}^{(c)} = \sum_{i=1}^H \sum_{j=1}^W s_{ij}^{(c)} \cdot y_i \quad (3)$$

where  $x_j$  and  $y_i$  denote the horizontal and vertical coordinates normalized to a fixed range (typically  $[-1, 1]$ ).

This pooling technique thus compresses high-dimensional spatial information into a compact and interpretable form, reducing the amount of input information the policy model need to process, while remaining end-to-end differentiable. Nevertheless, this does not guarantee that the the pooling method isolated the task-relevant info, nor that it will ignore strong visual cues that may act as distractors in OOD scenes. Indeed, we find that Spatial Softmax struggles to perform in OOD scenarios, even though it leads to a slight increase in ID scenes.

**TokenLearner** [39] dynamically selects a small number of informative tokens from the full set of visual tokens, thereby reducing computational complexity, while preserving feature-rich information. For this reason, it was integrated as part of RT-1 [3], for speeding up inference. Unlike static pooling operations, TokenLearner introduces learnable spatial attention maps that are conditioned on the input,

TABLE I: Summary of evaluated PVRs.  denotes models trained for robotics. Size is in images unless noted. Dataset acronyms – **IN**: ImageNet [38], **LVD**: LVD-142M [34], **K**: Kinetics [26], **E4D**: Ego4D [15] and **E4D+MNI** [31].

Model	Arch.	Objective	Dataset (Size)
MAE [17]	ViT-B/16	MIM	IN (1.2M)
VC-1 [31]	 ViT-B/16	MIM	E4D+MNI (5.6M <sup>†</sup> )
DINOv1 [6]	ViT-B/16	Self-Distillation	IN (1.2M)
iBOT [52]	ViT-B/16	MIM+Self-Distillation	IN (14M)
DINOv2 [34]	ViT-B/14	MIM+Self-Distillation	LVD (142M)
ViT [12]	ViT-B/16	Supervised	IN (14M)
CLIP [36]	ViT-B/16	V-L Contrastive	LAION (2B)
MoCov2 [8]	R-50	Contrastive	IN (1.2M)
DenseCL [47]	R-50	Local Contrastive	IN (1.2M)
SwAV [5]	R-50	Clustering	IN (1.2M)
VICRegL [2]	R-50	VICReg (global+local)	IN (1.2M)
VFS [49]	R-50	Self-Distillation (video)	K (240K <sup>*</sup> )
VIP [30]	 R-50	Value Function	E4D (5M <sup>†</sup> )
R3M [33]	 R-50	Time Contrastive+Language	E4D (5M <sup>†</sup> )

<sup>†</sup>Number of frames from videos. <sup>\*</sup>Number of videos.

allowing the model to adaptively select visual regions of interest.

Given an input feature map  $F \in \mathbb{R}^{H \times W \times D}$ , TokenLearner computes  $M$  attention maps  $A^{(m)} \in \mathbb{R}^{H \times W}$  using a lightweight module, typically an MLP or convolutional layers followed by a softmax over the spatial dimensions:  $A^{(m)} = \text{softmax}(\phi_m(F))$ , for  $m = 1, \dots, M$ , where  $\phi_m$  denotes the attention function for the  $m$ -th token.

Each learned token  $T^{(m)} \in \mathbb{R}^D$  is then computed as the weighted sum over spatial locations:

$$T^{(m)} = \sum_{i=1}^H \sum_{j=1}^W A_{ij}^{(m)} \cdot F_{ij} \quad (4)$$

The resulting set of tokens  $\{T^{(1)}, \dots, T^{(M)}\} \in \mathbb{R}^{M \times D}$  serves as a compact yet informative representation that can be passed to a Transformer encoder or a policy network.

In our framework, we compare AFA to TokenLearner by evaluating their capacity to isolate and preserve task-relevant visual cues. While both methods introduce adaptive pooling, we find that AFA further encourages robustness under visual scene perturbations.

#### IV. METHODOLOGY

We posit that training policies using the global features of PVRs (*i.e.*, CLS token for ViTs or average pooled channel feature for CNNs) can lead to overfitting to scene conditions that are irrelevant to the task at hand. The output features of these representations often capture visual characteristics of the scene that may be irrelevant to the policy (*e.g.*, the texture of a tabletop). Processing such extraneous information not only dilutes the policy network’s focus, but also leads to overfitting to scene specific conditions. This observation aligns with recent work on vision model evaluation [7], which argues that only specific image regions carry the necessary information for solving a task.

Building on this insight, we hypothesise that incorporating local information is particularly effective in the con-

text of robot learning, echoing findings in PVR distillation research [40], though this area remains empirically under-explored, particularly since token pooling methods are utilised for reducing the computational load, instead of filtering out irrelevant information that might drive the policy OOD.

Recognising the importance of local information is only part of the solution. A data-driven mechanism is also required to filter irrelevant details, such as background patches, and prioritise task-relevant information. To this end, we adopt the *attentive probing* methodology [7] in the context of visuomotor policy learning to implement *Attentive Feature Aggregation* (AFA). Specifically, we append a cross-attention layer to the frozen PVR, modified to include a trainable query token that interacts with the sequence of local tokens produced by the model. This token implicitly learns to *ask* the questions: “*where do I need to look to solve the task?*”. The local tokens correspond to the per-patch embeddings for ViTs and the channel embeddings for CNNs, both from the final layer. Consequently, we deploy:

$$AFA(\mathbf{q}, F) = \text{softmax} \left( \frac{\mathbf{q} \cdot (F \cdot W_K)^\top}{\sqrt{d_k}} \right) F \cdot W_V. \quad (5)$$

The trainable query token  $\mathbf{q}$  computes dot products with the feature sequence, with length equal to the number of patches and dimension  $d_k$ , organized as a matrix  $F$ . These dot products are passed through a softmax function to assign weights to the contributions of each local token to the final embedding. Our AFA module consists of multiple heads, so that specific dimension groups that might be irrelevant to the policy can be filtered out. Gradients are allowed to flow through the cross-attention layer, updating the parameters of  $\mathbf{q}$  as well as the key and value projection matrices,  $W_K$  and  $W_V$ . A visualisation of this approach is depicted in Fig. 3b.

## V. EXPERIMENTS

In this section, we introduce our experiments. First, in Section V-A we summarise our implementation details, regarding the used environment, choice of PVRs, policy training approach and AFA hyperparameters. Second, in Section V-B we analyse the ID and OOD performance of all PVRs raw and combined with different pooling methods. Third, in Section V-C, we rely on our insight from the robustness evaluation to introduce two metrics that act as strong OOD policy performance predictors. Finally, in Section V-D, we validate our findings in the real-world.

### A. Implementation Details

**Environment.** We conduct our experiments in the popular, MuJoCo-based [43] MetaWorld simulation environment [51]. We select ten tasks (namely: box-close-v2, disassemble-v2, shelf-place-v2, peg-insert-side-v2, bin-picking-v2, coffee-pull-v2, assembly-v2, drawer-open-v2, pick-place-wall-v2, button-press-wall-v2) and generate 25 expert demonstrations with a maximum of 175 rollout steps for each using the provided heuristic policies.

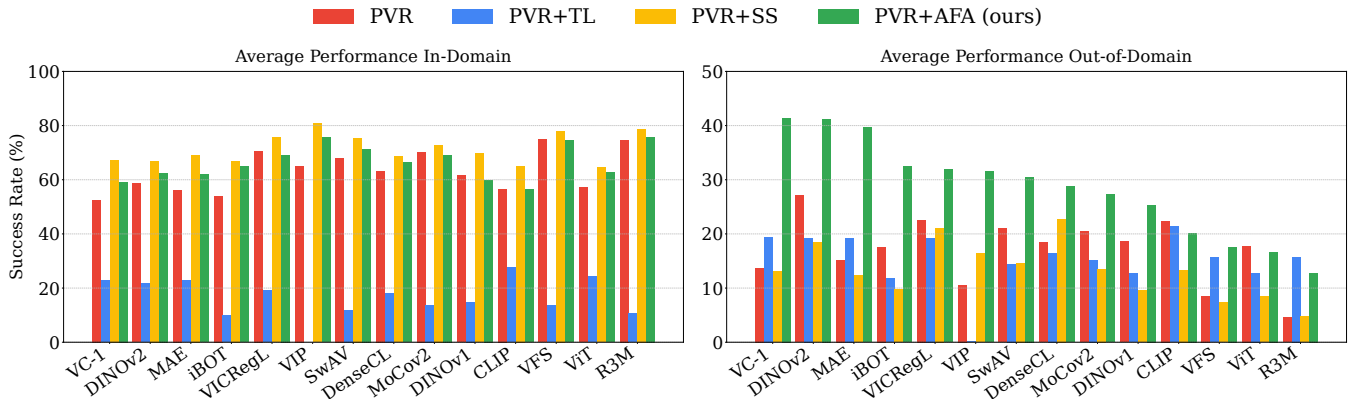


Fig. 4: Success rate (%) of policies trained with features from 14 PVRs in and out-of-domain. For **PVR**, the raw output PVR features are utilised (*i.e.*, CLS token for ViTs and the channel average for ResNets). **PVR+TL**, **PVR+SS**, and **PVR+AFA** stack a *TokenLearner*, a Spatial Softmax, and an *Attentive Feature Aggregation* pooling module after the PVR, respectively.

*Randomising the scene’s lighting properties.* The brightness of the scene is altered by adjusting the diffuse light components, where each colour channel (red, green, blue) is randomly set to a value between 0.3 and 1.0. The specular highlights are similarly randomized, with lower intensity values ranging from 0.1 to 0.5. Additionally, the position of each light source is varied randomly within a 3D space, spanning horizontal and vertical shifts between -2 and 2 units and height adjustments between 0.5 and 3 units. Lastly, the direction of the lights is randomized, allowing for changes in their angular orientation, with each directional component varying between -1 and 1 for horizontal/vertical angles and up to -1 for downward angles.

*Randomising the Tabletop’s texture.* We randomly modify the tabletop texture selecting from 30 distinct textures (some of which are borrowed from [48], visualised in the supplementary material). Some are visually similar to the texture used in the training demos and others are vibrant, with patterns that hold semantic information that could potentially attract the attention of a PVR. Nevertheless, by observing the evaluation rollouts, policies can fail and succeed in both out-of-distribution cases.

In Fig. 2 we visualise the used tasks and their corresponding visually perturbed versions.

**PVRs.** To validate our hypotheses, we test as vision encoders for training our policy seven Residual Networks (ResNets) [18] and seven Vision Transformers (ViT) [12], as summarised in Tab. I. Our selection includes the most popular PVRs utilised in robot learning applications that have led to SoTA performance. We also aim to ensure diversity across different training strategies, datasets, and the balance between local and global perception. The models tested include powerful representations from vision-specific approaches (*e.g.*, DINOV2 [34]), vision-language models (*e.g.*, CLIP [36]), and robot-learning-focused models (*e.g.*, R3M [33]). Despite these variations, we maintain a consistent backbone architecture of ResNet-50 or ViT-B/16, with the exception of DINOV2 [34], which employs a smaller patch size of 14. Also, for DINOV2 we discard overlapping

patches, to ensure fairness in the comparison of PVRs. The models tested include powerful representations from vision-specific approaches (*e.g.*, DINO [6]), vision-language models (*e.g.*, CLIP [36]), and robot-learning-focused models (*e.g.*, R3M [33]).

**Policy training.** We repeat each policy training five times using different seeds, keeping the PVR frozen, and report the interquartile mean (IQM) success rate. We train with mini-batches of 128 samples for 80K steps.

**AFA.** We use a cross-attention layer with 12 heads for ViT features and 32 heads for ResNet features. This configuration ensures that we process 64-dimensional feature chunks in both cases, maintaining fairness between the two backbone architectures. Consistent with standard attentive probing methodologies [7], [10], we employ a cosine learning rate scheduler with a warm-up phase. TE is applied to augment features with a temporal component and specifically for AFA, the temporal feature is concatenated with the output of the cross-attention module.

## B. Policy Robustness Evaluation

To evaluate robustness, we compare four distinct approaches both in ID and OOD scenarios. First, we train policies directly with global PVR features (annotated as PVR). The remaining three policies all aggregate local features using different methods: PVR+TL uses TokenLearner, PVR+SS employs Spatial SoftMax, and PVR+AFA utilizes Attentive Feature Aggregation (ours). We summarise the performance of each policy category in Fig. 4, averaged across tasks and perturbation types in the OOD case. From these results, several trends emerge.

First, AFA yields the best OOD performance, in many cases even tripling the success rate (*e.g.*, VC-1, MAE, VIP, etc.). The only exceptions are three from the worse performing PVRs: CLIP, ViT and R3M. Regarding, the first two, no pooling method outperforms the raw PVR case. This is reasonable, as these models are trained with objectives that emphasise global frame perception, unlike other models that incorporate supervision at the patch level.

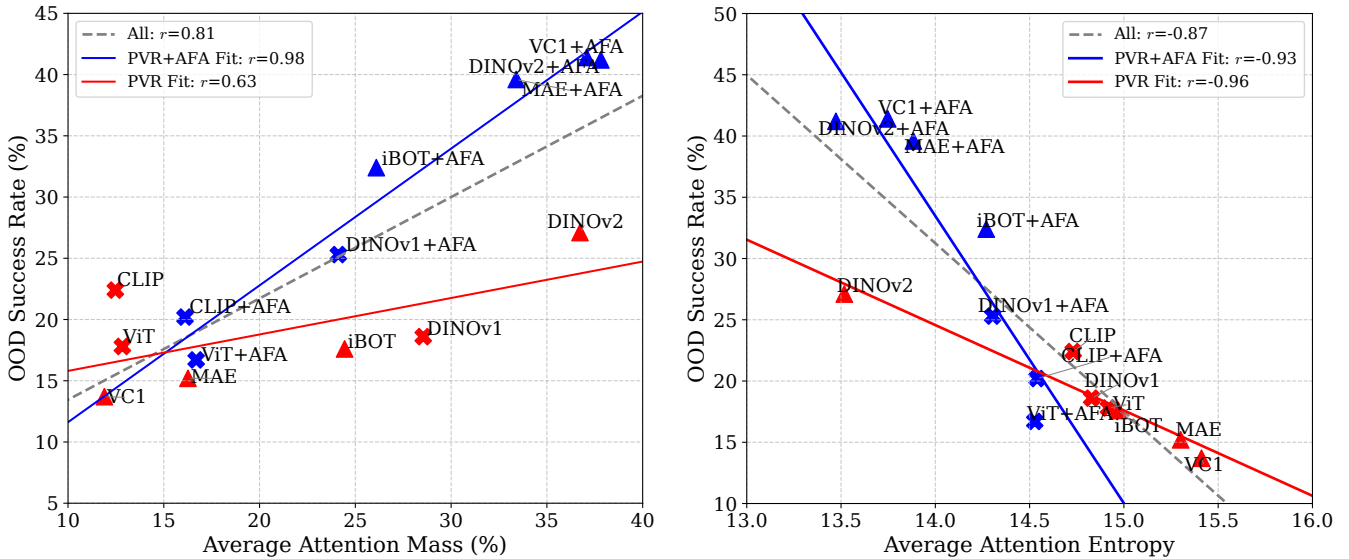


Fig. 5: Correlation plots for the OOD performance predictors. On the left, we visualise how the greater the attention mass percentage that falls within the masks of task-relevant areas (*e.g.*, robot, object, target location, etc.) the more likely it is for the corresponding PVR to lead to a higher OOD policy success rate. Similarly, on the right, the entropy of the attention (*i.e.*, how targetted the attention is) is strongly and negatively correlated with OOD performance. Both plots visualise with red the results from raw PVR features, with blue the results from AFA-filtered features and with gray the overall trend.

For the case of R3M, PVR+TL leads to slightly higher policy success rate. Notably, MIM-trained PVRs (*i.e.*, VC-1, DINOv2, MAE and iBOT) benefit the most from AFA, reflecting the alignment between AFA’s design, which is inspired by attentive probing, and the training principles of MIM-based models. These findings highlight AFA’s ability to enhance policy performance, particularly in challenging OOD scenarios, and underscore its compatibility with models that leverage local feature representations.

Second, the average in-domain performance remains nearly unchanged between PVR and PVR+AFA, with a slight increase from 63.1% to 66.4% in the latter approach. The minor boost observed with AFA in in-domain scenarios, especially when compared to its substantial improvements in perturbed scenes, suggests that AFA does not learn a new latent space for the PVR, more suited to the task. Instead, it appears to refine the use of the existing latent space by learning to leverage relevant information while discarding elements that are irrelevant to the policy. This distinction underscores AFA’s role as a mechanism for better utilisation of pre-trained features rather than redefining or adapting the underlying feature space. Furthermore, PVR+SS seems to lead to a slight boost in ID performance, compared to both PVR and PVR+AFA, but this performance is not retained in the OOD evaluation, where in all but three encoder choices (*i.e.*, VIP, DenseCL and R3M) PVR+SS demonstrated notably degraded performance even to the raw PVR-trained policies. Finally, PVR+TL seems to perform poorly both in the ID and OOD cases.

Overall, we argue that the reduced performance of PVR+SS and PVR+TL in OOD scenes is not surprising. TokenLearner operates on feature level, ignoring the

information structure that is encoded per attention head. Its convolution-based spatial gating tends to learn rigid, location-dependent patterns, making it sensitive to changes in spatial arrangement, while it also lacks a content-based mechanism to adaptively focus on the most relevant information. Additionally, Spatial Softmax does not try to favour specific visual cues, but rather compresses the image information. As a result, redundant cues that are unrelated to the task remain. On the other hand, AFA learns to linearly transform the tokens and then combines them with unique weights per token head.

### C. OOD Performance Predictors

We find two trends among PVRs that lead to high OOD policy success rates and provide evidence that AFA enhances these attributes. All examined trends concern the attention maps extracted from the studied ViTs, utilising the provided expert demos. First, we measured the average attention mass that falls within the robot arm and objects of interaction. For this, we extracted the masks using SAMv2 [37]. We find very strong positive correlation ( $\rho = 0.81$ ) between this metric and the OOD performance and observe that AFA magnifies this behaviour (see left plot of Fig. 5). Second, we measure how much targetted the attention is, by computing the entropy of the attention heatmap. We find very strong negative correlation ( $\rho = -0.87$ ) between the entropy and the OOD success rate (see right plot of Fig. 5). Similarly to before, AFA enhances this behaviour, as visualised in Fig. 1, where attention appears to be extremely focused. Consequently, AFA seems to successfully learn to attend to task-relevant visual cues, ignoring changes in the scene (*e.g.*, semantically rich distractor objects).

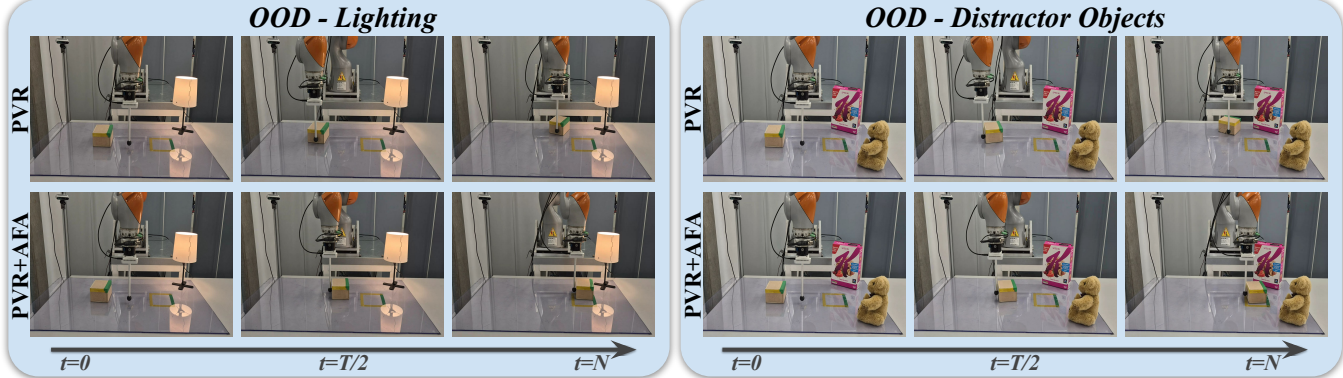


Fig. 6: Real-world evaluation comparing rollouts for a planar pushing task from a PVR (top row) and our PVR+AFA (bottom row) trained policy. We visualise two cases: (i) lighting changes, and (ii) distractor objects. All results are available in the project page.

#### D. Real-World Experiments

We also validated the efficacy of AFA in the real-world. We selected a simple planar pushing task, where the goal is for the robot to push a cube inside of a marked outline on the table, matching the colour of each side. The robot can only move on the  $(x, y)$  plane to push the cube, using a rod that has been attached to the end-effector. We collected 20 demonstrations via teleoperation with the KUKA IIWA 14 robot and a RealSense D415 camera that observes the workspace. We executed the trained policies using a NVIDIA GeForce RTX 2080, generating a new action at 10Hz. We utilised features extracted from DINOv1 [6], which we empirically observed performed better at the particular task compared to other models.

We pre-trained for 0.2M steps a policy model with and without AFA, using the 20 collected demonstrations. Both models had no problem solving the task in-domain. Nevertheless, under visual perturbations, the policy trained with the raw PVR output was unable to push the cube within the outline on the table, in many cases performing actions that seemed random. On the other hand, when trained with AFA, using the per patch tokens, the policy exhibited robustness, solving all the tasks with distractors and lighting changes. We visualise two OOD examples in Fig. 6 (more can be found in the video and project page) and report the success rate in Table II.

TABLE II: Real-world success rate. We shift the scene OOD by adding random distractors to the scene, changing the lighting conditions and by modifying the manipulated object.

In-Domain	Distractors	Lighting	Object
PVR	4/5	0/4	0/3
PVR + AFA	4/5	4/4	3/3

## VI. DISCUSSION

In this work, we demonstrated that the robustness of visuomotor policies leveraging PVRs is critically dependent not just on the encoder itself, but on how its features are

aggregated. Our proposed AFA offers a simple yet powerful method to learn to focus on task-relevant visual cues, significantly improving OOD performance without the need for costly dataset augmentation or PVR fine-tuning. This finding suggests a promising path toward more deployable robotic systems that can operate reliably in visually dynamic environments.

Nevertheless, a question naturally arises: “*which PVR characteristics are most suitable for robot learning?*”, particularly in OOD scenes. From the selected PVRs, the models that were developed with visuomotor policy learning as the target application were: VIP, VC-1 and R3M. However, this does not seem to be the most important characteristic for achieving high success rate and robustness. Similarly, whether the backbone of the PVR is a CNN or a vision transformer seems to be playing a small role. In-domain, VFS and R3M score the highest performance (close to 80%), but this is most likely due to their temporal perception. On the other hand, OOD performance seems to depend mostly on the MIM-training strategy when combined with AFA, and not on the training dataset (*e.g.*, if it’s static or from video). This is not unreasonable, given the powerful local perception that this methodology leads to. Similarly, these observations highlight that we are still to uncover an optimal approach for building vision encoders for policy learning.

## REFERENCES

- [1] Adrien Bardes, Quentin Garrido, Jean Ponce, Michael Rabbat, Yann LeCun, Mahmoud Assran, and Nicolas Ballas. Revisiting feature prediction for learning visual representations from video. *arXiv:2404.08471*, 2024.
- [2] Adrien Bardes, Jean Ponce, and Yann LeCun. Vicregl: Self-supervised learning of local visual features. *NeurIPS*, 2022.
- [3] Anthony Brohan, Noah Brown, and et al. Rt-1: Robotics transformer for real-world control at scale. In *RSS*, 2023.
- [4] Kaylee Burns, Zach Witzel, Jubayer Ibn Hamid, Tianhe Yu, Chelsea Finn, and Karol Hausman. What makes pre-trained visual representations successful for robust manipulation? In *CoRL*, 2024.
- [5] Mathilde Caron, Ishan Misra, Julien Mairal, Priya Goyal, Piotr Bojanowski, and Armand Joulin. Unsupervised learning of visual features by contrasting cluster assignments. *NeurIPS*, 2020.
- [6] Mathilde Caron, Hugo Touvron, Ishan Misra, Hervé Jégou, Julien Mairal, Piotr Bojanowski, and Armand Joulin. Emerging properties in self-supervised vision transformers. In *ICCV*, 2021.

[7] Xiaokang Chen, Mingyu Ding, Xiaodi Wang, Ying Xin, Shentong Mo, Yunhao Wang, Shumin Han, Ping Luo, Gang Zeng, and Jingdong Wang. Context autoencoder for self-supervised representation learning. *IJCV*, 2024.

[8] Xinlei Chen, Haoqi Fan, Ross Girshick, and Kaiming He. Improved baselines with momentum contrastive learning. *arXiv preprint arXiv:2003.04297*, 2020.

[9] Cheng Chi, Siyuan Feng, Yilun Du, Zhenjia Xu, Eric Cousineau, Benjamin Burchfiel, and Shuran Song. Diffusion policy: Visuomotor policy learning via action diffusion. In *RSS*, 2023.

[10] Duolikun Danier, Mehmet Akgün, Changjian Li, Hakan Bilen, and Oisin Mac Aodha. DepthCues: Evaluating Monocular Depth Perception in Large Vision Models. In *CVPR*, 2025.

[11] Sudeep Dasari, Mohan Kumar Srirama, Unnat Jain, and Abhinav Gupta. An unbiased look at datasets for visuo-motor pre-training. In *CoRL*, 2023.

[12] Alexey Dosovitskiy, Lucas Beyer, Alexander Kolesnikov, Dirk Weissenborn, Xiaohua Zhai, Thomas Unterthiner, Mostafa Dehghani, Matthias Minderer, Georg Heigold, Sylvain Gelly, Jakob Uszkoreit, and Neil Houlsby. An image is worth 16x16 words: Transformers for image recognition at scale. In *ICLR*, 2021.

[13] Chelsea Finn, Xin Yu Tan, Yan Duan, Trevor Darrell, Sergey Levine, and Pieter Abbeel. Deep spatial autoencoders for visuomotor learning. In *ICRA*, 2016.

[14] Letian Fu, Huang Huang, Gaurav Datta, Lawrence Yunliang Chen, William Chung-Ho Panitch, Fangchen Liu, Hui Li, and Ken Goldberg. In-context imitation learning via next-token prediction. In *ICRA*, 2025.

[15] Kristen Grauman, Andrew Westbury, and et al. Ego4d: Around the world in 3,000 hours of egocentric video. In *CVPR*, 2022.

[16] Nicklas Hansen, Zhecheng Yuan, Yanjie Ze, Tongzhou Mu, Aravind Rajeswaran, Hao Su, Huazhe Xu, and Xiaolong Wang. On pre-training for visuo-motor control: Revisiting a learning-from-scratch baseline. In *ICML*, 2023.

[17] Kaiming He, Xinlei Chen, Saining Xie, Yanghao Li, Piotr Doll’ar, and Ross B. Girshick. Masked autoencoders are scalable vision learners. *CVPR*, 2022.

[18] Kaiming He, Xiangyu Zhang, Shaoqing Ren, and Jian Sun. Deep residual learning for image recognition. In *CVPR*, 2016.

[19] Neil Houlsby, Andrei Giurgiu, Stanislaw Jastrzebski, Bruna Morrone, Quentin De Laroussilhe, Andrea Gesmundo, Mona Attariyan, and Sylvain Gelly. Parameter-efficient transfer learning for NLP. In *ICML*, 2019.

[20] Kyle Hsu, Tyler Ga Wei Lum, Ruohan Gao, Shixiang Shane Gu, Jiajun Wu, and Chelsea Finn. What makes certain pre-trained visual representations better for robotic learning? In *Deep Reinforcement Learning Workshop NeurIPS 2022*, 2022.

[21] Yingdong Hu, Renhao Wang, Li Erran Li, and Yang Gao. For pre-trained vision models in motor control, not all policy learning methods are created equal. In *ICML*, 2023.

[22] Huang Huang, Fangchen Liu, Letian Fu, Tingfan Wu, Mustafa Mukadam, Jitendra Malik, Ken Goldberg, and Pieter Abbeel. Otter: A vision-language-action model with text-aware feature extraciton. *arXiv*, 2025.

[23] Wenlong Huang, Chen Wang, Ruohan Zhang, Yunzhu Li, Jiajun Wu, and Li Fei-Fei. Voxposer: Composable 3d value maps for robotic manipulation with language models. *CoRL*, 2023.

[24] Ya Jing, Xuelin Zhu, Xingbin Liu, Qie Sima, Taozheng Yang, Yunhai Feng, and Tao Kong. Exploring visual pre-training for robot manipulation: Datasets, models and methods. In *IROS*, 2023.

[25] Yuanchen Ju, Kaizhe Hu, Guowei Zhang, Gu Zhang, Mingrun Jiang, and Huazhe Xu. Robo-abc: Affordance generalization beyond categories via semantic correspondence for robot manipulation. In *ECCV*, 2025.

[26] Will Kay, Joao Carreira, Karen Simonyan, Brian Zhang, Chloe Hillier, Sudheendra Vijayanarasimhan, Fabio Viola, Tim Green, Trevor Back, Paul Natsev, Mustafa Suleyman, and Andrew Zisserman. The kinetics human action video dataset, 2017.

[27] Sergey Levine, Chelsea Finn, Trevor Darrell, and Pieter Abbeel. End-to-end training of deep visuomotor policies. *Journal of Machine Learning Research (JMLR)*, 2016.

[28] Gen Li, Nikolaos Tsagkas, Jifei Song, Ruaridh Mon-Williams, Sethu Vijayakumar, Kun Shao, and Laura Sevilla-Lara. Learning precise affordances from egocentric videos for robotic manipulation. *arxiv preprint arXiv:2408.10123*, 2024.

[29] Xingyu Lin, John So, Sashwat Mahalingam, Fangchen Liu, and Pieter Abbeel. Spawnnnet: Learning generalizable visuomotor skills from pre-trained network. In *ICRA*, 2024.

[30] Yecheng Jason Ma and et al. VIP: Towards universal visual reward and representation via value-implicit pre-training. In *ICLR*, 2023.

[31] Arjun Majumdar, Karmesh Yadav, and et al. Where are we in the search for an artificial visual cortex for embodied intelligence? In *NeurIPS*, 2023.

[32] Octave Mariotti, Oisin Mac Aodha, and Hakan Bilen. Improving semantic correspondence with viewpoint-guided spherical maps. In *CVPR*, 2024.

[33] Suraj Nair, Aravind Rajeswaran, Vikash Kumar, Chelsea Finn, and Abhinav Gupta. R3m: A universal visual representation for robot manipulation. In *CoRL*, 2022.

[34] Maxime Oquab, Timothée Darct, Theo Moutakanni, Huy V. Vo, Marc Szafraniec, Vasil Khalidov, Pierre Fernandez, Daniel Haziza, Francisco Massa, Alaaeldin El-Nouby, Russell Howes, et al. Dinov2: Learning robust visual features without supervision. *TMLR*, 2024.

[35] Simone Parisi, Aravind Rajeswaran, Senthil Purushwalkam, and Abhinav Gupta. The (un)surprising effectiveness of pre-trained vision models for control. In *ICML*, 2022.

[36] Alec Radford, Jong Wook Kim, Chris Hallacy, Aditya Ramesh, Gabriel Goh, Sandhini Agarwal, Girish Sastry, Amanda Askell, Pamela Mishkin, Jack Clark, et al. Learning transferable visual models from natural language supervision. In *ICML*, 2021.

[37] Nikhila Ravi and et al. SAM 2: Segment Anything in Images and Videos. In *ICLR*, 2025.

[38] Tal Ridnik and et al. Imagenet-21k pretraining for the masses. In *Advances in Neural Information Processing Systems Track on Datasets and Benchmarks*, 2021.

[39] Michael S Ryoo, AJ Piergiovanni, Anurag Arnab, Mostafa Dehghani, and Anelia Angelova. Tokenlearner: Adaptive space-time tokenization for videos. In *NeurIPS*, 2021.

[40] Jinghuan Shang, Karl Schmeckpeper, Brandon B. May, Maria Vittoria Minniti, Tarik Kelestemur, David Watkins, and Laura Herlant. Theia: Distilling diverse vision foundation models for robot learning. In *CoRL*, 2024.

[41] William Shen, Ge Yang, Alan Yu, Jansen Wong, Leslie Pack Kaelbling, and Phillip Isola. Distilled feature fields enable few-shot language-guided manipulation. In *CoRL*, 2023.

[42] Sneha Silwal, Karmesh Yadav, Tingfan Wu, Jay Vakil, Arjun Majumdar, Sergio Arnaud, Claire Chen, Vincent-Pierre Berges, Dhruv Batra, Aravind Rajeswaran, Mrinal Kalakrishnan, Franziska Meier, and Oleksandr Maksymets. What do we learn from a large-scale study of pre-trained visual representations in sim and real environments? In *ICRA*, 2024.

[43] Emanuel Todorov, Tom Erez, and Yuval Tassa. Mujoco: A physics engine for model-based control. In *IROS*, 2012.

[44] Nikolaos Tsagkas, Oisin Mac Aodha, and Chris XiaoXuan Lu. Vi-fields: Towards language-grounded neural implicit spatial representations. In *International Conference on Robotics and Automation Workshops (ICRA)*, 2023.

[45] Nikolaos Tsagkas, Jack Rome, Subramanian Ramamoorthy, Oisin Mac Aodha, and Chris XiaoXuan Lu. Click to grasp: Zero-shot precise manipulation via visual diffusion descriptors. In *IROS*, 2024.

[46] Nikolaos Tsagkas, Andreas Sochopoulos, Duolikun Danier, Sethu Vijayakumar, Chris XiaoXuan Lu, and Oisin Mac Aodha. On the use of pre-trained visual representations in visuo-motor robot learning. In *6th Embodied AI Workshop CVPR*, 2025.

[47] Xinlong Wang, Rufeng Zhang, Chunhua Shen, Tao Kong, and Lei Li. Dense contrastive learning for self-supervised visual pre-training. In *CVPR*, 2021.

[48] Annie Xie and et al. Decomposing the generalization gap in imitation learning for visual robotic manipulation. In *ICRA*, 2024.

[49] Jiarui Xu and Xiaolong Wang. Rethinking self-supervised correspondence learning: A video frame-level similarity perspective. In *ICCV*, 2021.

[50] Lihe Yang, Bingyi Kang, Zilong Huang, Zhen Zhao, Xiaogang Xu, Jia Shi Feng, and Hengshuang Zhao. Depth anything v2. In *Advances in Neural Information Processing Systems*, 2024.

[51] Tianhe Yu and et al. Meta-world: A benchmark and evaluation for multi-task and meta-reinforcement learning. In *CoRL*, 2020.

[52] Jinghao Zhou, Chen Wei, Huiyu Wang, Wei Shen, Cihang Xie, Alan Yuille, and Tao Kong. ibot: Image bert pre-training with online tokenizer. In *ICLR*, 2022.